RESEARCH ARTICLE

Personalized brain stimulation for effective neurointervention across participants

Nienke E. R. van Bueren[1,2‡], **Thomas L. Reed**[1‡], **Vu Nguyen**[3,6], **James G. Sheffield**[1], **Sanne H. G. van der Ven**[2], **Michael A. Osborne**[4], **Evelyn H. Kroesbergen**[2], **Roi Cohen Kadosh**[1,5]*

1 Wellcome Centre for Integrative Neuroimaging, Department of Experimental Psychology, University of Oxford, Oxford, United Kingdom, 2 Behavioural Science Institute, Radboud University Nijmegen, Nijmegen, the Netherlands, 3 Department of Materials, University of Oxford, Oxford, United Kingdom, 4 Department of Engineering Science, University of Oxford, Oxford, United Kingdom, 5 School of Psychology, Faculty of Health and Medical Sciences, University of Surrey, Guildford, United Kingdom, 6 Amazon, Adelaide, Australia

‡ These authors share first authorship on this work.
* r.cohenkadosh@surrey.ac.uk

Abstract

Accumulating evidence from human-based research has highlighted that the prevalent one-size-fits-all approach for neural and behavioral interventions is inefficient. This approach can benefit one individual, but be ineffective or even detrimental for another. Studying the efficacy of the large range of different parameters for different individuals is costly, time-consuming and requires a large sample size that makes such research impractical and hinders effective interventions. Here an active machine learning technique is presented across participants—personalized Bayesian optimization (pBO)—that searches available parameter combinations to optimize an intervention as a function of an individual's ability. This novel technique was utilized to identify transcranial alternating current stimulation (tACS) frequency and current strength combinations most likely to improve arithmetic performance, based on a subject's baseline arithmetic abilities. The pBO was performed across all subjects tested, building a model of subject performance, capable of recommending parameters for future subjects based on their baseline arithmetic ability. pBO successfully searches, learns, and recommends parameters for an effective neurointervention as supported by behavioral, simulation, and neural data. The application of pBO in human-based research opens up new avenues for personalized and more effective interventions, as well as discoveries of protocols for treatment and translation to other clinical and non-clinical domains.

Author summary

The common one-size-fits-all approach used in biological and behavioral research has shown to be inefficient. This is especially the case in the field of brain stimulation, where many different combinations of stimulation parameters (i.e., frequency and current strength of the applied current) can be used for restorative or enhancement purposes, in clinical and non-clinical populations, respectively. Even intervention protocols that have

reported to be effective for certain individuals can be detrimental for others. Here we present an active machine learning method, personalized Bayesian optimization (pBO) that successfully searches, learns, and recommends neurostimulation parameters across individuals. Based on an individual's baseline cognitive ability, the pBO identifies specific combinations of transcranial alternating current stimulation parameters, which are most likely to improve cognitive performance, in which case arithmetic problem solving. This timely approach provides a possible solution for the pressing need for personalization in different disciplines including medicine, psychology, and education.

Introduction

There is no doubt that the human organism is complex, and the impact of nature and nurture, as well as their interaction, increases variability between humans. It is therefore not surprising that interventions aimed at altering human behavior are not effective for all individuals. This variability in effectiveness is partly due to the one-size-fits-all approach that currently dominates behavioral intervention research. Accumulating evidence has indicated that this approach is inefficient, and that a treatment that benefits one individual can be ineffective or even detrimental for another individual [1–8]. Personalized medicine aims to address this challenge by adjusting treatments to the individual or to a subset of patients [9,10]. Due to the complexity of individual differences, there is an increasing need for personalized medicine for a wide range of drugs, biomedical treatments, and diseases. Without this, the one-size-fits-all approach often only alleviates symptoms in clinical studies without curing the disease [11]. This demand for personalization is especially true in the field of transcranial stimulation, where electrical currents targeting specific brain regions are used to alter behavior. Whilst tailoring a stimulation protocol is ideal, identifying the optimal stimulation protocol for an individual proves problematic in large parameter spaces, where the systematic testing of each parameter combination can lead to overly costly and time-consuming protocols. For instance, one stimulation technique that is gaining popularity is transcranial alternating current stimulation (tACS) [12]. tACS utilizes an alternating current delivered via multiple electrodes placed on the scalp, which is capable of propagating through the scalp and modulating the activity of the underlying neurons. The applied alternating current promotes oscillatory activity at the stimulation frequency [13], allowing direct modulation of brain oscillations that subserve cognitive processes [14]. Through this process, tACS provides an attractive way to investigate causal predictors of behavior and to use such knowledge to improve human capabilities or health. However, exploring the effects of all tACS parameters on the performance of different individuals requires an exhausting amount of testing when considering different current (0–2 mA) and frequency (0–100 Hz) combinations.

One recently proposed method for selecting parameters in brain stimulation is Bayesian optimization (BO) [15,16]. BO is an active machine learning technique that aims to find the global optimum of a black-box function $f(x)$ by making a series of evaluations. To select the next evaluation, BO first constructs a probabilistic model (surrogate model) for $f(x)$ and exploits this model to make decisions. This results in a procedure that can find the maximal value of difficult non-concave functions with relatively few evaluations, at the cost of performing more computations to determine the next point (at minimal cost when compared with the effort of evaluating the function at more points) [17]. Hence, BO is particularly valuable when there is a need to explore a large experimental space in as few evaluations as possible. Generally, BO involves two procedures: 1) fitting an appropriate model to function $f(x)$ and 2)

choosing an acquisition function α(x) that steers sampling in the direction where improvement over the current best evaluation is most likely. It should be mentioned that other brain state-dependent stimulation methods that included personalized real-time electrophysiological (EEG) correlates show promising results [18].

The present work was inspired by previous work that used BO in human-based research [15,16,19–21]. In these previous BO studies, all iterations of the process are run on the same individual, allowing the experimenters to achieve person-specific results. However, to do this, the entire BO process must be run for each individual that requires stimulation—a lengthy and costly process. A workable solution is to base the algorithm on a measurable characteristic that varies across subjects, such as baseline ability in the behavioral task of interest. Therefore, we developed a novel personalized (p)BO for human-based research. In pBO, the algorithm is trained on an initial small set of data (burn-in phase), and then iteratively selects stimulation parameters across subsequent subjects, with the aim of identifying the optimal stimulation parameters for improving behavioral performance, whilst considering personalized information. i.e. baseline arithmetic ability (**Fig 1**).

This BO algorithm can incorporate personalized information [22], including an individual's data, such as age, gender, neural activity or cognitive profile. Based on the vast literature that highlights the impact of individual differences on stimulation efficacy [23,24], we personalized the BO to subject's cognitive ability in this study. We focused on optimizing arithmetic performance considering its importance in the success of one's future career and socio-economic status [25] and its impairment in acquired and congenital brain disorders [26]. Skills needed for solving arithmetic problems vary greatly in the typical and atypical populations [27,28]. Similarly, a recent study on arithmetic skills highlighted the individual differences in both neural correlates and behavioral response in healthy people [29]. The left frontoparietal network has been implicated in playing an important role in arithmetic processing and can be targeted by tACS [30,31]. We recognize that other brain stimulation techniques have been used in the field of arithmetic [32–37], for reviews see [31,38,39]. However, we utilized tACS since this method allows for stimulation at a range of specific frequencies to explore those that might impact arithmetic performance.
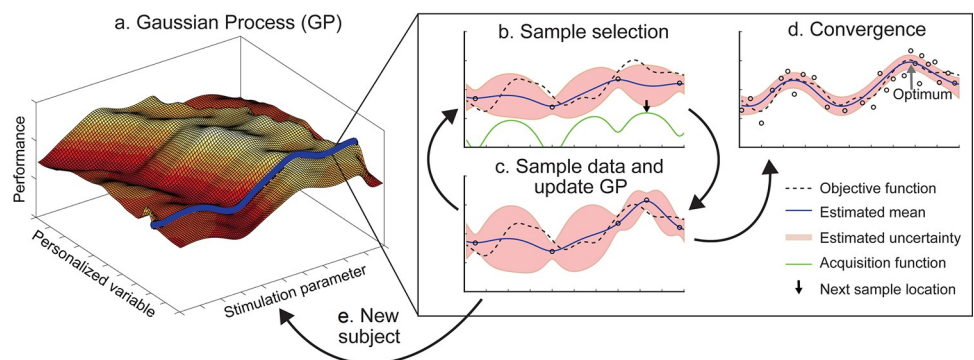
Fig 1. Illustration of the personalized Bayesian optimization procedure of theoretical values. a) The Gaussian process (GP) is fitted to the existing data and models the expected performance along parameter and personalized dimensions. **b)** The acquisition function identifies the next point to evaluate along the value of the personalized variable relevant to the participant. **c)** Once the data is collected at this new point the GP is updated and a new point selected. **d)** This cycle continues until either a new subject is tested, in which case a different value for the personalized variable will be recorded. **e)** a pre-set stopping criterion is reached, such as the number of subjects to be tested; or until the potential improvement is considered negligible (convergence). In this study, we utilized a pre-set stopping criterion of 50 subjects, after which testing was ceased.

We examined whether we could tailor tACS parameters to improve arithmetic performance using a pBO that takes baseline ability into account in healthy subjects. To do this, the individual's baseline arithmetic ability was initially measured, after which the stimulation parameters to be used were automatically selected either at random, if subjects were in the initial burn-in phase (initialization phase), or by the pBO algorithm. Subjects then completed a block of the arithmetic behavioral task whilst receiving stimulation using the selected parameters (Fig 2). Stimulation parameter selection and behavioral testing were repeated in each subject until three blocks of different arithmetic problems were completed. Note that these three blocks were included to select more samples to allow optimization based on the pBO across subjects, rather than optimizing performance over these three iterations. The tACS parameters that were altered were current intensity and frequency, and the pBO algorithm aimed to identify the optimal parameter combination for improving arithmetic ability given a subject's baseline arithmetic ability. To target the ability to solve arithmetic problems more precisely we used diffusion modeling, which allowed us to incorporate human performance while taking into account measures of both accuracy and reaction time in its calculation, a measure of cognitive ability, rather than auxiliary components such as non-decision response time or response conservativeness [40]. Furthermore, we ran different computational simulations to demonstrate the efficiency of our proposed pBO in comparison to random sampling and a standard BO algorithm (i.e., pBO without a personalized variable). We also recorded electrophysiological
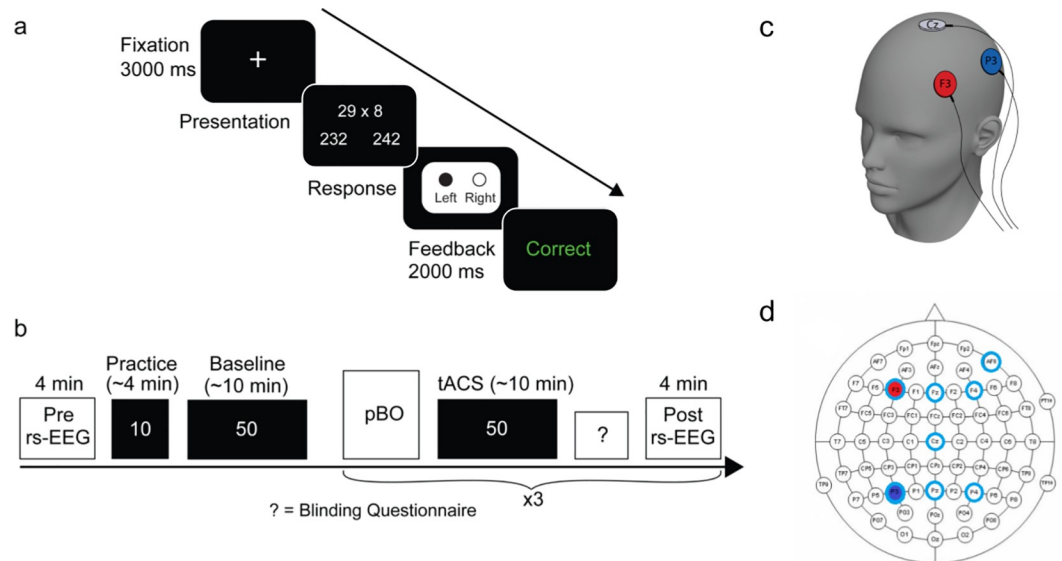
Fig 2. An overview of the experimental paradigm. a) An overview of the behavioral paradigm. Subjects (n = 50) watched a fixation point that indicated the start of a trial. After 3000 ms an arithmetic multiplication was shown with two possible answer options on the left and right side with a difference of 10 to keep consistency in task difficulty. Subjects responded by pressing either the left or right button on a response box as quickly and accurately with no time limit present. Lastly, subjects received either 'correct' or 'incorrect' as feedback to continuously capture attention. **b)** Subjects first completed a baseline rs-EEG of four minutes, after which 10 practice trials of multi-digit times single-digit multiplications were presented of four minutes. This was followed by the baseline task of 10 minutes, which comprised five blocks of 10 different multiplications. Subjects had a short break (~3 minutes) between baseline and the pBO. Three different tACS frequency-current combinations were proposed by the pBO algorithm after the completion of each sequence of 50 trials of the multiplication task which was approximately 30 minutes in total. Between these tACS combinations, post-block rs-EEGs of four minutes were recorded before the subjects moved on to the next tACS combination. Validation of the blinding of the stimulation and perceived sensations were assessed after completion of a stimulation block. **c)** An illustration of the tACS electrode montage. Stimulation was applied over the left frontoparietal area (F3 and P3) with one return electrode (Cz). **d)** A top down topoplot showing both the stimulation electrodes (red and blue) and the EEG electrode placing (turquoise).

frequency band power and connectivity at baseline and after applying combinations of tACS parameters to link behavioral changes to EEG outcomes, while we report this finding, we note that it is not the main focus of the present study.
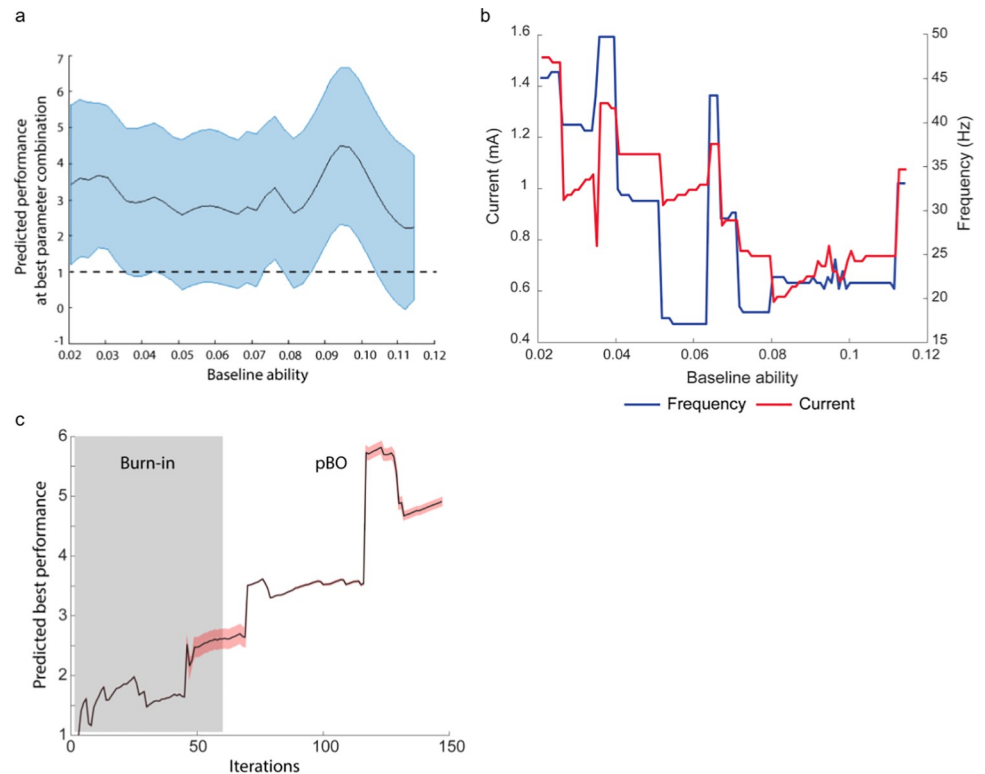
Results

Personalized Bayesian optimization

Baseline ability is a continuous parameter and it should be considered that the best inferred tACS combination differs along this continuum. Following the suggestion of Aiken, West, and Reno [41] to allow for further visual inspection, we visualized the continuum at three different points: low (mean -1 SD), mean and high (mean +1 SD) baseline ability. As **Fig 3** shows, the optimal stimulation parameters depended on the participants' baseline ability: we found a shift from higher frequencies and currents in lower (poor) baseline abilities, to lower frequencies and currents in higher (better) baseline abilities (mean - 1SD (38.67 Hz, 0.97 mA), mean (16.67 Hz, 0.88 mA), mean + 1SD (18 Hz, 0.6 mA), mA values are peak-to-peak).
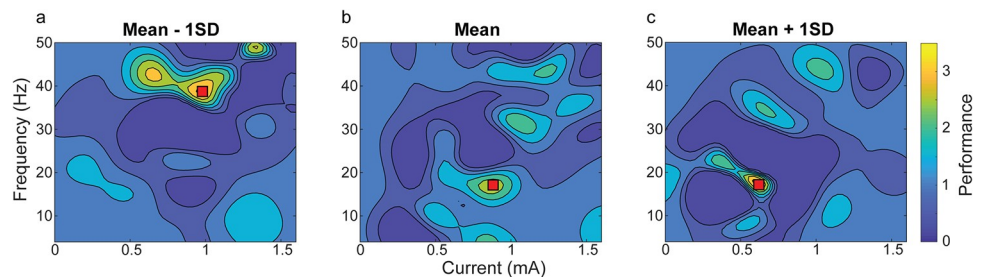
Fig 3. Results of the personalized Bayesian optimization model at several different baseline abilities (n = 49). The figure shows the predictions from the Gaussian process model for low baseline ability (panel a: 1 standard deviation (SD) below the mean), mean baseline ability (panel b: mean = 0.055), and for high baseline ability (panel c: 1 SD above the mean). The y-axis shows the frequency range of the applied stimulation (0–50 Hz) and the x-axis the current of the stimulation (0–1.6 mA, peak-to-peak). Arithmetic performance is indicated in color based on the normalized drift rates (tACS block/baseline block). Low drift rates are shown in dark blue and high drift rates in yellow. A best-inferred point for arithmetic performance according to a specific frequency-current combination is indicated by a red square in all three panels. Note that this figure is not based on different groups of participants as in moderation analysis, but represents a three dimensional view of the GP's surrogate surface at three different points for visualization purposes.

A more in-depth visualization of the efficacy of the pBO procedure revealed that the overall fluctuation in performance improvement (e.g., normalized to the baseline performance without stimulation) across subjects with low and high baseline abilities was similar (**Fig 4A**). This result indicates that the success of our approach is equally effective for people with either low or high arithmetic baseline ability. The optimal frequency-current tACS parameter combinations proposed by the pBO algorithm confirms a shift from higher frequencies and currents in low-baseline ability subjects to lower frequencies and currents when baseline ability increases (**Fig 4B**; see also **Fig 3**). The behavior of the pBO algorithm can be seen in **Fig 4C** as the predicted best performance dramatically increases a number of times over the course of one iteration. This is where a beneficial stimulation combination is identified. Further, the predicted best performance tends to decrease soon after as that point is retested, and a more accurate estimation of the performance is identified. The best performance predicted by the GP was calculated as the highest value (i.e. "the best") that the GP predicted across the frequency-current combinations. In addition, the black-box function $f(x)$ is reliably optimized over the course of the iterations, as shown by an increase in the individual's ability to solve arithmetic problems (**Fig 4C**).

Fig 4. Results of optimizing behavior with personalized Bayesian optimization (pBO) (n = 49). a) In-depth visualization of the normalized performance according to baseline ability during pBO. Normalized performance was calculated as the drift rate of the performance block divided by the drift rate of the baseline block. Subjects on the lower part of the baseline ability spectrum showed a similar arithmetic performance improvement during tACS compared to subjects on the higher baseline ability spectrum. Note that a normalized performance score of 1 indicates no difference with baseline arithmetic performance when no stimulation was applied. A normalized performance score higher than 1 indicates improved performance as measured with drift rate. The blue shaded area indicates 95% credibility intervals. **b)** The change in frequency-amplitude tACS parameters proposed by the pBO algorithm based on the individualized baseline ability in arithmetic at the end of optimization. **c)** Predicted best performance at each iteration (i.e., different blocks), calculated as the best performance predicted by the GP at any parameter combination. Subjects were added sequentially, with three subsequent iterations were assessed for each participant. For example, iterations 148–150, represents blocks 1–3 for the 50th subject. Surrogate uncertainty is shown by the shaded area in pink. Note that during some iterations uncertainty is higher due to new baseline abilities introduced in the pBO and due to outliers. These outliers are retested later which then reduces uncertainty.

https://doi.org/10.1371/journal.pcbi.1008886.g004

Based on the suggestion of one of the anonymous reviewers, we also performed cross-validation as a resampling procedure to evaluate our pBO algorithm on a limited data sample. We performed cross-validation by randomly splitting 80% of the participants into a training group and the remaining 20% into a testing group. In this regression problem, the input included the current intensity, frequency and baseline ability. The output was the performance score in drift rate. The aim was to estimate how the model was expected to perform in general when used to make predictions on data not used during the training of the model. Using the Gaussian process for regression, we measured the Mean Squared Error (MSE) which is the average error between the true value against the predicted value. The results of this analysis showed an MSE of 0.3 for this validation task. To put this MSE score into context, the (arithmetic) performance score from this experiment ranges from 0.5 to 3.8 with a standard deviation of 0.54. We can see that the MSE of 0.3 is reasonable given the unavoidable measurement noise which is common in the field of experimental psychology.

Personalized Bayesian optimization simulation analysis

To demonstrate the efficiency of our proposed pBO, we examined the optimization performance on a Hartmann 3-dimensional function [42]. This 3-dimensional function is a suitable benchmark representing our real experiments including three variables (frequency, current, and baseline ability). When running a Hartmann 3-dimensional optimization using the expected improvement (EI) [43] as an acquisition function in the pBO algorithm, the pBO algorithm outperformed a standard BO algorithm as well as random sampling (**Fig 5**). Whilst this is a comparison of a model with 3 parameters (pBO) outperforming a model with 2 parameters (BO), this simulates the additional data incorporated into the pBO model in the form of a relevant personalized variable, which is not present in standard BO. The results of this comparison show that higher drift rate values are attained more quickly when using the EI pBO procedure in comparison with BO and random sampling (**Fig 5A**), and the pBO algorithm was shown to identify an optima closer to the true optima of the Hartmann function (**Fig 5B**). When the noise variance σ_n^2 increases, the pBO performance is closer to the performance of random sampling and standard BO (**Fig 5**). As further mentioned in section 'Acquisition function' relating to hyperparameter considerations, the estimate of σ_n^2 from our observed data which varies by iterations ranged between 0.01 and 2.

Thus, if the behavioral evaluations of the experimental procedure are too noisy, the pBO procedure's ability to make correct judgements about the optimum parameters is diminished but it is still able to outperform random sampling. Critically, as **Fig 5** illustrates within these estimated noise variance ranges, our pBO leads to improved optimization compared with the standard BO approach that does not take baseline ability into account. In particular, the standard BO is unable to enhance performance, thus highlighting the benefit of personalization vs. the one-size-fits-all approach.

Baseline electroencephalography and arithmetic ability

To examine whether our results are supported by neurophysiology we used baseline electroencephalography (EEG). Previous EEG studies suggest a positive relationship between left frontoparietal theta (4–8 Hz) connectivity and high-level cognitive processing [44–48]. However, none was found when running a regression model trying to predict baseline arithmetic ability from baseline left frontoparietal connectivity in the theta range (all $p > .3$). The same applied to frontal theta power ($p = .88$), theta/beta ratio, and beta (14–30 Hz) connectivity (all $p > .1$). However, our findings from the pBO models highlight an optimal performance effect in the beta frequency range (14–30 Hz) in subjects with average and high baseline ability, whilst low baseline ability individuals benefit from stimulation in the gamma frequency range (> 30 Hz). We therefore examined the relationship between baseline ability and baseline frontal beta power in an exploratory manner. Higher (gamma) frequencies could not be recorded reliably with the equipment. We found that subjects with higher arithmetic baseline ability have higher baseline beta power in comparison to subjects with lower arithmetic baseline skills (non-parametric (Spearman) correlation: $r_s = .29$, $p = .03$). This neurophysiological finding corroborates the group-level pBO model results, where the pBO algorithm chose the tACS frequency that mirrors baseline neurophysiological activity in those individuals.

Discussion

Most interventions in humans are not tailored to the individual's characteristics, such as behavior or brain function, but use a one-size-fits-all approach that leads to inefficient or even ineffective interventions [1–8]. This lack of progress is rooted mainly in the complexity of
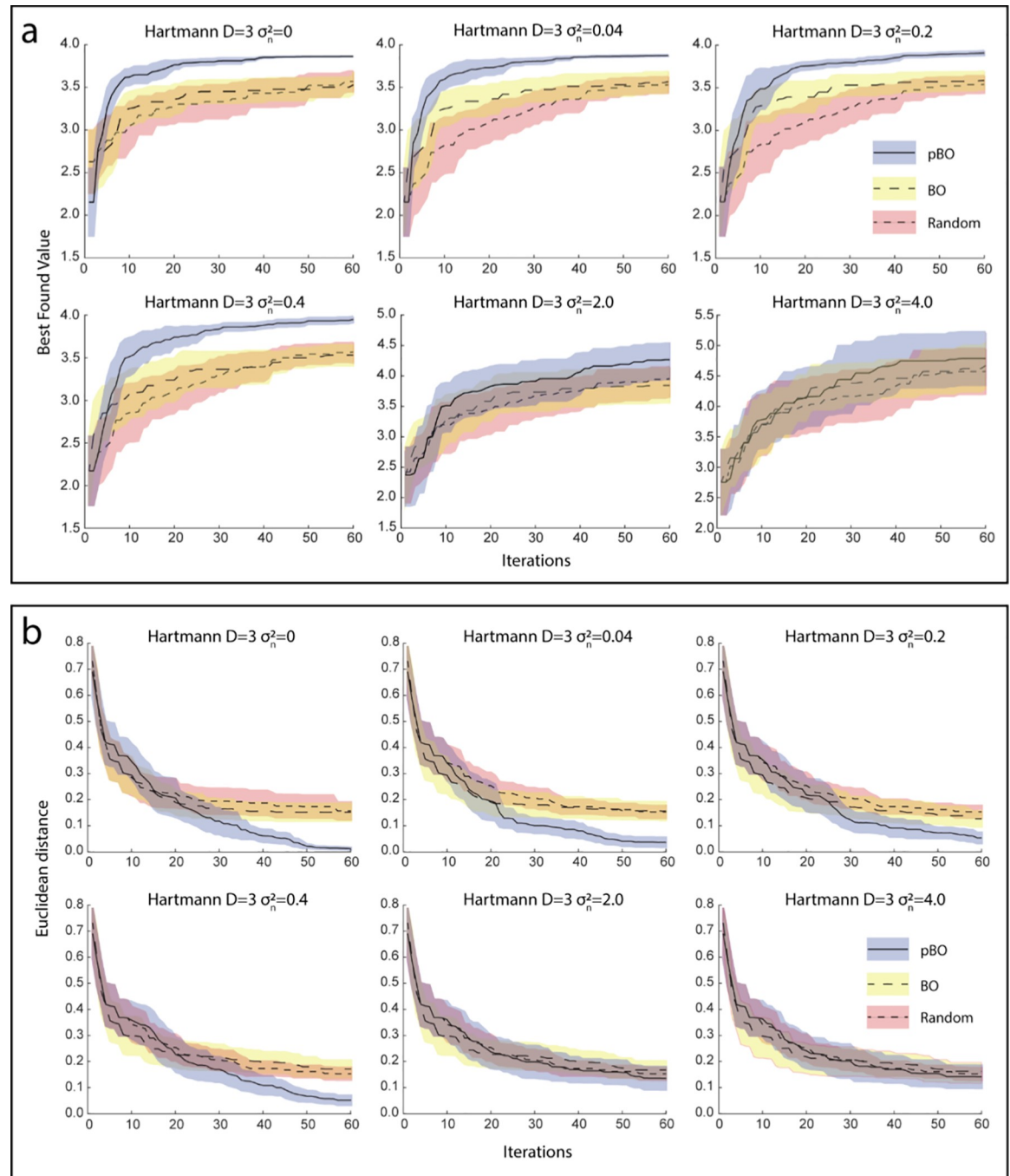
Fig 5. Results of simulating the ability of pBO, BO and random search algorithms on identifying the optima in the Hartmann 3-dimensional surface. The simulation was run 30 times on each of the six different levels of noise, lines represent the mean performance and shaded areas the standard deviation of 30 repeats. **a)** Shows the best found value identified by each algorithm at each iteration, demonstrating that the pBO algorithm is able to find higher values more quickly than the BO and random search algorithms. **b)** Shows the Euclidean distance of the identified optima from the true optima of the Hartmann function (i.e., accuracy of the algorithm). The pBO algorithm is shown to be more accurate than the BO and random search algorithms, except at very high levels of noise, where they are comparable.

personalizing interventions, due to the immense burden on time and resources. The results of the empirical and simulation experiments performed in the present study demonstrate that our pBO algorithm is capable of tailoring different current strengths and frequencies of tACS to an individual's baseline ability. Specifically, we demonstrated that the optimal stimulation parameters, determined by the pBO algorithm, differ in low and high arithmetic baseline individuals. This suggests that there are either different cognitive processes involved or differing effects of stimulation in these groups. For example, a recent multiplication study indicated possible behavioral constraints of a one-size-fits-all brain stimulation protocol on performers in a certain subgroup of the population (e.g., high performers) [48]. Notably, the present results cannot be explained by a placebo (sham) stimulation, as we controlled for placebo effects of stimulation by including 0 mA in the search space of the pBO algorithm, as well as other very weak currents that are assumed to be ineffective. In addition, if our effects could be explained by a placebo effect, it should have led to the parameters that yielded the strongest sensation, which was not the case (**S2** and **S4 Figs**). Similarly, our results cannot be attributed to the participants learning effects as improvement in arithmetic performance was based on an improvement across participants, and not within.

Highlighting the significance of our results, the majority of previous brain stimulation studies that aimed to determine stimulation parameters have only tested a small number of different parameters to observe their differential effects [31]. However, this approach leaves a large amount of stimulation parameter combinations unexplored, as such exploration is both expensive and time consuming. Whilst a small number of studies have utilized BO, they have focused on running the entire BO paradigm on one individual to find their best stimulation parameters [15,16]. This approach, while providing many advantages, does not allow for the convenient transfer of parameters optimized for one subject to new subjects, and does not allow its usage in contexts that do not permit repeated sampling in the same individual due to ethical constraints, potential side effects, or time pressure. Additionally, the need to sample to the parameter space during the initial burn-in phase increases the sample size required to identify optimal stimulation parameters. In contrast, our pBO algorithm provides further advancements by including the following novel processes. Firstly, our algorithm receives personalized data, in this study baseline cognitive data from a subject, and suggests the stimulation parameters to test that are conditioned on the baseline data. Due to the ability to recommend personalized stimulation parameters solely based on a baseline measure, our work on a pBO algorithm represents a significant advance in this area. To illustrate, our experimental findings demonstrate that pBO preferentially selects more successful tACS parameters to optimize the interventional outcome, in this case arithmetic performance (**Fig 4**). Secondly, our study shows that non-personalized interventions, as in standard BO, are ineffective due to the inability to optimize performance effectively (**Fig 5**). Our simulations further show that pBO is reliable even when there is a considerable amount of noise present in the models. Previously, most BO applications have been in a noise-free context, in contrast with human-based studies that are prone to noisy evaluations. More precisely, as noise increases, the pBO algorithm is less able to evaluate the stimulation parameters correctly, but still outperforms random sampling and the standard BO algorithm. This furthermore applies to the estimated noise variance ranges that were observed from our data.

In addition, the behavioral and simulation results support our electrophysiological evidence that pBO can provide new protocols for intervention as well as mechanistic insights. In the present study, pBO highlighted the importance of frontal beta frequencies (14–30 Hz) as indicated by the BO group-level model in subjects with average and high arithmetic abilities. In line with our group-level pBO models, we showed that high baseline ability subjects have higher frontal beta power in comparison with low baseline ability subjects. In addition, subjects with low baseline abilities benefit more from tACS in the gamma frequency range, which is in line with responses

linked to spike timing dependent plasticity (STDP) [49]. However, gamma frequencies could not be recorded reliably with EEG due to low-pass filtering properties of the skin and skull together with a low signal-to-noise ratio [50], and was therefore not statistically explored. This limitation can be overcome by magnetoencephalography (MEG), as was shown by a study indicating frequency-specific neural entrainment by tACS [51]. The overlap of our pBO model with the baseline EEG correlates provides a causal inference of the involvement of baseline oscillatory brain activity (notably beta activity) in mathematics performance, a relation that was only known to be correlational in the field of mathematical cognition until now [31,52].

One constraint of this approach that should be considered, is that the distribution of subject baseline abilities in this study was weighted towards the lower end of the ability range, leading to fewer subjects with higher baseline ability being tested (**S1 Fig**). Therefore, results in the lower baseline ability spectrum are of higher confidence regarding an estimation of the optimum frequency-current tACS combination. This notion is especially relevant on account of the similar results in our group-level pBO model for the mean and high baseline abilities. Additionally, the subjects that participated were mainly university (under)graduates, which might have led to a small arithmetic ability range when compared to the population. A possibility exists that our pBO models will differ slightly when testing more subjects with higher baseline abilities. Moreover, while we demonstrated the personalization of intervention based on two dimensions (i.e., the current and frequency of tACS) and a personalized feature, our algorithm allows for the inclusion of many more dimensions (e.g., phase, brain region, and duration of stimulation) in future interventions. Additionally, the personalized variables are pervasive in human-based research and can include multiple variables such as behavioral data, neural activity, age, and gender. For example, the presented findings could translate to other neurointerventions, such as other forms of transcranial electrical stimulations, transcranial magnetic stimulation (TMS) or to sensing-enabled brain stimulation such as deep brain stimulation (DBS) and the responsive neurostimulation system (RNS). Similar to tACS, these interventions use a broad range of stimulation parameters whereby it is uncertain which parameters are more successful to optimize the interventional outcome due to individual differences in healthy subjects or patients [53–55]. Our pBO approach overcomes this limitation by personalizing the intervention based on the selection of stimulation dimensions together with a personalized feature. Taken together, the use of our pBO approach is widely applicable, and can simultaneously model multiple dimensions together with a wide range of choices of personalized variables. Further investigations into closed-loop algorithms for individualized interventions may greatly improve the reliability of those interventions. This is particularly important in a clinical setting where the aim is to optimize symptom improvement.

To conclude, we have demonstrated a more efficient research process, taking as a working model the field of brain stimulation to overcome the problem of selecting stimulation parameters for each individual. The method we suggest here can be extended with minimal or no changes to different fields in which the optimal parameters are unknown and/or expensive to assess, including drug discovery, invasive and non-invasive brain stimulation, and physical and mental training in both typical and atypical populations.

Methods

Subjects and ethics statement

Fifty subjects gave written consent before the start of the study. All met the safety criteria for transcranial electrical stimulation (tES) and received financial compensation of £20. In addition to this compensation, subjects had the chance of winning an additional £50 based on their performance (the winner was randomly drawn from the best 10 performers over the three

blocks). Behavioral data from all 49 subjects aged between 18–30 years old (31 of whom were female) were used for the pBO (mean age = 22.52 ± standard deviation (SD) = 4.09). All were right-handed. One completed their education at GCSE level, 14 at A-level, 17 were undergraduates and 18 were postgraduates. In the UK educational system GCSE refers to secondary education and A-level refers to an advanced level that can lead to university. All subjects reported no contraindications to electrical stimulation or any history of dyscalculia, dyslexia or attentional deficits. The proposed study received ethical approval from The University of Oxford Medical Sciences Interdivisional Research Ethics Committee (protocol number: MSD-I-DREC-C2-2014-033). Additionally, we pre-registered the present study on the Open Science Framework; see https://osf.io/bg2pd.

Overview of experimental paradigm and stimuli

The study was conducted in an electrically shielded lab space at the University of Oxford, where environmental influences (i.e., lighting, seating, EEG cap) were kept constant throughout the experiment. Over the course of the experiment, subjects completed four blocks of fifty multiplication problems—one baseline block and three stimulation blocks (see **Fig 2**). After recording an initial 4-minute baseline resting state EEG, the task was explained to the subjects and they completed 10 practice trials of approximately 4 minutes, followed by the baseline block of 10 minutes during which no tACS was administered. In each block, subjects had to indicate which answer was correct as accurately and as fast as possible with no time limit present (see **Fig 2A**). Subjects indicated the correct answer by pressing either the left or the right button on a response box situated in front of them. They underwent three blocks of multiplications of 30 minutes in total in which they received tACS. Prior to each tACS block, the pBO algorithm was run (<5 seconds) to determine the stimulation parameters (current intensity and frequency) to be delivered during the upcoming experimental block based on the individual subject's performance in the baseline block. The stimulation parameters were automatically selected by the algorithm and administered whilst maintaining blinding in both the subject and experimenter (for a complete list of the applied current and frequency, see **S1** and **S2 Tables**). Rs-EEG of 4 minutes was recorded again after each stimulation block. Note that the stimulation electrodes were integrated in the EEG cap which allowed us to use the same electrodes for both EEG recording and stimulation.

Behavioral stimuli

Arithmetic performance was tested using an arithmetic calculation paradigm, consisting of problems involving a single-digit number multiplied by a two-digit number, with a three-digit outcome. This paradigm was presented using Matlab's psychtoolbox version 3. A calculation paradigm was used instead of a retrieval paradigm since calculation has been associated with an increased activation in the frontoparietal network [30,56,57]. None of the multiplications included operands with the digits 0, 1, or 2 to prevent variations in difficulty. In addition, the two-digit operand was not smaller than 15, did not use repeated digits, and was not a multiple of 10. Subjects were visually presented with a multiplication problem on a screen with a correct and incorrect answer positioned under the multiplication problem on the left and right side. The position of the correct and incorrect answer was randomly allocated to the right and left sides of the screen and they always differed by 10. Each problem was presented only once, and their order was randomized.

Measurement of baseline abilities

An arithmetic baseline task containing 50 different arithmetic multiplications was presented to measure individual arithmetic ability in terms of response times and accuracy.

Subsequently, baseline drift rates were calculated for each subject according to the two-choice EZ-diffusion model [40]. This approach allowed us to dissect the different components in the chain of information processing by modeling the decision process and targeting the cognitive component of interest (the drift rate, which reflects ability and task difficulty by modeling response time and accuracy), rather than auxiliary components [40,58]. This model was chosen to combine reliably the response time and accuracy in one outcome that could be optimized through the pBO procedure. The 50 trials completed in the baseline block were randomly divided into two sets, and for both sets a separate drift rate was calculated. One was used as a measure of the subject's baseline ability, whilst the other was used to normalize the drift rates calculated during the optimization phase (e.g., during the experimental procedure of the pBO). This was done to eliminate dependency between the subject's baseline ability score and the normalized score in each stimulation block [59]. To reduce fatigue, subjects had a break of 30 s after every 10 trials. After completing the baseline task, subjects had a short break (~3 minutes) before they continued with the experimental procedure of the pBO.

Experimental procedure of the pBO

Before the start of the pBO procedure, a burn-in phase was used that consisted of 60 random tACS parameters assigned to the first 20 subjects to initiate the pBO procedure. The pBO code (i.e., coded stimulation parameters, for example, 1 mA and 10 Hz has been coded as 320) was manually initiated before each performance block and took <5 seconds to run. The stimulation parameters selected by the algorithm, based on an individual's baseline ability, were automatically saved and passed to the stimulation software to maintain double blinding. The pBO algorithm selected stimulation parameters for the subject, with the aim of improving behavioral performance given their baseline ability. This was done in an iterative process across 30 subjects, with the algorithm's estimate of the optimal stimulation parameter, at any given baseline ability, becoming more accurate as more subjects were tested. At each run of the pBO algorithm, all previously collected data was used, including data collected in the burn-in phase and the GP was refitted to model all the data. As we *a priori* defined in our preregistration, we utilized a pre-set stopping criteria of 50 subjects, after which testing was ceased.

Our rationale to set the sample size to 50 subjects was as follows: For BO without noise [60], n = 10–20 per dimension is often used. For BO with noise, a recent work set the number of evaluations to 25 per dimension [61]. However, to take into account the possibility that we might deal with increased noise in the present study, we set it to n = 50 per dimension (50 subjects x 3 blocks each, equals 150 evaluations to account for three dimensions (frequency, current, and baseline ability).

In total, 150 diverse multiplication problems (three blocks of 50 trials) were administered during the experimental procedure. After each block, performance drift rates were calculated immediately, another rs-EEG was measured for four minutes, and then for the next block the combination of tACS parameters (frequency and current) was changed. Thus, behavioral performance optimization relied on the frequency and current of tACS together with the baseline cognitive ability as indicated by the drift rate. Each subject received three different frequency-current tACS combinations.

Transcranial alternating current stimulation

The alternating current stimulation was administered over the left frontoparietal network (see **Fig 2C**). The tACS was delivered via two stimulation (3.14 mm diameter) NG Pistim Ag/AgCl electrodes (F3 and P3) with one return electrode (Cz) using the Starstim 32 (Neuroelectrics, Barcelona). The conductive interface used was electrode gel Signagel. The impedances of the

electrodes were held at < 10 kΩ. The stimulation intensity ranged between 0.1–1.6 mA peak-to-peak in steps of 0.1 for the burn-in phase of the study. For the optimization phase, 0 mA was added to control for possible sham influences. We chose the maximum stimulation intensity based on a small pilot study on three subjects to determine the maximum comfortable intensity. Different combinations of frequencies in the range from 5–50 Hz and intensity in the range from 0–2 mA peak-to-peak were tested. Subjects indicated by means of verbal communication their highest tolerable intensity, where 1.6 mA was chosen as the maximum intensity. The stimulation frequency ranged between 5–50 Hz in steps of 1 Hz for the whole experiment.

Stimulation was administered in a double-blind manner during the three experimental blocks with a maximum of 10 minutes for each block. Stimulation started 45 s before the start of the block and changed after every block. If the subjects received a stimulation intensity of 0 mA during a block (sham stimulation), a ramp-up and a ramp-down of 30 s was initiated to provide the initial skin sensations during stimulation to ensure blinding. When the subject completed a block within 10 minutes, stimulation was ramped down for 30 s and the subject proceeded to the four-minute rs-EEG. Note that in cases where subjects completed the task in under 10 minutes, they did not receive the full length of stimulation. These stimulation blocks did not differ from the stimulation block in which the subject received the full length of stimulation except for performance. Twenty-four of the 150 stimulation blocks had a duration of less than 10 minutes but more than 7.50 minutes, and 126 stimulation blocks had a duration of more than 10 minutes. This posed no problem, since the present study only investigated the online effects of tACS on arithmetic behavior. After completing a block related to one tACS combination, the subjects filled out a questionnaire in which they were asked several questions designed to gauge the level of sensation experienced during stimulation (see S1 Questionnaire Items). We used this data to assess the relationship between the intensity rating of every sensation and tACS amplitude.

Resting state-EEG recordings and pre-processing

Resting state-EEG recordings were made at the start of the study (before baseline measurements) and immediately after every stimulation block. Electrophysiological data were obtained with eight gel Ag/AgCl electrodes (F3, P3, F4, P4, Fz, Cz, Pz, AF8) according to the international 10/10 EEG system using the wireless Starstim R32 sensor system (Neuroelectrics, Barcelona, Spain), with no online filters. The conductive interface used was electrode gel Signagel. The ground consisted of adhesive active common mode sense (CMS) and passive driven right leg (DRL) electrodes which were positioned on the right mastoid. All EEG measurements had a duration of four minutes in which the subjects had their eyes open while watching a fixation point in the middle of the screen. Raw EEG data were recorded and used for offline analysis using EEGLAB 13.6.5b [62], which is an open source toolbox running on Matlab R2018b [63]. Data were high-pass filtered at 0.1 Hz, and low-pass filtered at 50 Hz (using a finite impulse response filter). Visual inspection was carried out to remove artefacts caused by muscle movement. We rejected an EEG recording from analysis if more than 25 percent of the data in a given block were removed. This resulted in the EEG data from four stimulation blocks being rejected (2% of the data). Independent component analysis was used to remove blinks and noisy components. On average, 1.23 ± 0.62 SD components were rejected per subject, with a maximum of three components and a minimum of zero.

Note that our EEG recording and preprocessing pipeline was unsuited to analyzing gamma frequency activity for a number of reasons. Firstly, we used a conservative pipeline to ensure the removal of noise from our data instead of removing relevant brain activity. Additionally,

the short recording time of 4 minutes used in this study is inadequate to reliably measure gamma activity [64], as well as the unavoidable use of resting recordings leading to a lack of task-evoked gamma peak, which would be much more reliably detected than resting state [65]. However, we would like to reinstate that the EEG outcomes are not the main focus of the present study.

Sensation analysis

In line with a previous study [66], and as stated in our pre-registration, we expected higher sensitivity ratings of the tACS parameters with higher current values compared with lower currents. Therefore, we predicted a positive correlation between the intensity rating for itching, pain, burning, phosphenes, warmth, and fatigue. We performed a separate correlation analysis to calculate the bivariate Pearson's coefficient (r) or Spearman's rho (r_s) depending on normality to assess the relationship between the intensity of different sensations induced by tACS and height of tACS current (**S2** and **S4** **Figs**).

Bayesian optimization

Bayesian optimization uses *f* to denote an unknown objective function (e.g., black-box function) for which we do not have a closed-form expression, but we could have an infinite number of queries. Furthermore, this black-box function is expensive and time costly to evaluate. Formally, let *f*: $X \rightarrow R$ (R is the set of all real numbers, representing the values from $-\infty$ to $+\infty$) be a well-behaved function, defined on a subset $X \subseteq R^d$ whereby d is the number of dimensions. The standard BO approach is aimed at solving the following global optimization problem:

$$\boldsymbol{x}^* = \arg\max_{x \in X} f(x) \tag{1}$$

The BO algorithm is aimed at finding the global optimum of arithmetic performance, as indicated by drift rates, of the black-box function $f(x)$ by making a series of evaluations at x_1, $x_2, \ldots, x_T$ (see S1 Mathematical Variables).

Personalized Bayesian optimization

While our approach could personalize a given treatment based on any individual characteristic, such as neural or biometric data, we chose cognitive ability, as the literature provides more supporting evidence for its moderating effect [1–3,7,8,46,67], especially as it is closely related to our desired behavioral outcome. Each subject has their individual arithmetic baseline ability: this value is considered as the personalized value. We needed to measure this value *p* separately for every subject, as was done during the baseline task. We expected to see that the optimal parameters will vary with different baseline abilities. That is, the optimal parameter x^* depends on the different values of *p*. For this reason, the standard BO presented in the previous section may not have been appropriate. Therefore, we proposed to solve the following optimization problem, defined formally as:

$$\boldsymbol{x}^*(p) = \arg\max_{x \in X} f(x, p) \tag{2}$$

where *p* is the baselines ability given for each subject. The optimal parameter x^* is not defined globally, but specifically to a variable *p*. This is the key difference of our pBO in comparison with the standard BO, while we acknowledge related research in BO with environmental variables [21,68,69].

Objective function

In the present tACS study, we used the following objective function $f(x,p)$:

$$f(x, p) = \frac{Vstim}{Vbase}$$

where $Vstim$ is the drift rate during the 50 trials of an arithmetic multiplication block normalized by the $Vbase$ (the drift rate calculated over 25 random trials from the baseline task). To determine improvement between the baseline and the stimulation block, a second $Vbase$ was calculated over the other 25 trials from the baseline task. A Pearson correlation was calculated to determine if the two drift rates from the baseline and the one used for the improvement index are related ($r = 57$, p < .001). The acquisition functions are carefully designed to allow a trade-off between exploration of the search space and the exploitation of current promising regions. A burn-in phase of 60 random tACS frequency-current combinations was used. These were assigned to the first 20 subjects of the BO design to determine the amount of variation induced by stimulation. We decided to use a large burn-in in our paradigm to design a reliable BO algorithm that was based on a large amount of data.

Personalized Gaussian process for joint modeling of target function and baseline ability

Standard BO models f with a GP, $f \sim GP(m, k)$, where m is the mean function and k is the covariance function [69]. This flexible distribution allowed us to associate a normally distributed random variable at every point in the continuous input space. Therefore, we obtained the predictive distribution for $\boldsymbol{f}$ at a new observation x that also follows a Gaussian distribution. Its mean (μ) and variance (σ^2) are given by:

$$\mu(x') = k(x'; X)K(X; X)^{-1}y$$

$$\sigma^2(x') = k(x'; x') - k(x'; X)K(X; X)^{-1}k(x'; X)^T \tag{3}$$

where $K(U; V)$ is a covariance matrix whose element $(i; j)$ is calculated as $k_{i,j} = k(x_i; x_j)$ with $x_i \in U$ and $x_j \in V$. Behavioral observations are typically associated with noise that can be accommodated in a GP model. Namely, every $f(x)$ processes extra variance due to independent noise:

$$y_i = f(x_i) + \epsilon_i \text{ where } \epsilon_i \sim N(0, \sigma_n^2) \text{ and } \sigma_n^2 \text{ is the noise variance.} \tag{4}$$

When considering noise, the output follows the GP as $y \sim GP(m, k + \sigma_n^2 \delta_{i,j})$, where $\delta_{i,j} = 1$ if $i = j$ is the Kronecker's delta. The covariance function for a noisy process becomes the sum of the signal covariance and the noise covariance. Specifically, the exponentiated-quadratic covariance function between two observations can be computed as:

$$k\left(x_i; x_j\right) = exp\left(-\frac{(x_i - x_j)^2}{2\sigma_l^2}\right) + \sigma_n^2 \delta_{i,j} \tag{5}$$

For a more elaborate overview of GPs, we refer the interested reader to Rasmussen and Williams [70].

In our personalized setting, one of the possible solutions is to build a GP and optimization for each value p. However, such a simplistic approach faces a critical problem of data efficiency, because the number of data samples is not sufficient to estimate each value p separately. Therefore, we extended the GP surrogate to jointly model our target function f and the

additional personalized dimension p, rather than using a separate GP for every subject. Specifically, the GP covariance becomes:

$$k(\{x_i, p_i\}; \{x_j, p_j\}) = k(x_i, x_j) \times k(p_i, p_j) \tag{6}$$

where $k(x_i, x_j)$ is defined in Eq (5) and $k\left(p_i, p_j\right) = exp\left(-\frac{(p_i - p_j)^2}{2\sigma_p^2}\right)$. These covariance functions correspond to the parameters and baselines, respectively. We note that the length scale parameter σ_p^2 used in $k(p_i, p_j)$ is different from σ_x^2 used in $k(x_i, x_j)$. For example, if the baseline ability length-scale σ_p^2 is extremely large, it means the performance is not changing with respect to the baseline performance. On the other hand, if σ_p^2 is small, it means the performance function is changing rapidly with the baseline performance. We later maximized the marginal likelihood to estimate these length scale parameters directly from the data [70]. Under our modification for the GP, we could estimate the predictive mean and predictive variance:

$$\mu(x, p) = k(\{x, p\}; Z)K(Z; Z)^{-1}y$$

$$\sigma^2(x, p) = k(\{x, p\}; \{x, p\}) - k(\{x, p\}; Z)K(Z; Z)^{-1}k(\{x, p\}; Z)^T \tag{7}$$

Where we denoted $Z = [X, P]$, the personalized covariance matrix k is defined in Eq (6).

Acquisition function

To select the next point to evaluate, the acquisition function $\alpha(x)$ was chosen to construct a utility function based on the GP surrogate model mentioned above. Instead of maximizing the expensive original function f, we maximized the cheaper acquisition function to select the next most optimal point:

$$\boldsymbol{x_{t+1}} = arg\max_{x \in X} \alpha(x)$$

In this auxiliary maximization problem, the acquisition function form is known and can be easily optimized by standard numerical techniques. One of the most common choices for the acquisition function is the GP upper confidence bound (GP-UCB):

$$\alpha(x, p) = \mu(x, p) + \kappa \times \sigma(x, p)$$

where $\mu(x, p)$ and $\sigma(x, p)$ are the GP predictive mean and variance defined in Eq (7) and κ is the hyperparameter controlling the exploration-exploitation trade-off. One can follow Srinivas et al. to specify the value of κ to achieve the theoretically-guaranteed performance [69]. The second common acquisition function is the expected improvement (EI) [43]. The EI finds the next sampling point given the highest chance of expectation to improve upon the best-found value so far. Using the analytical expression of Gaussian distribution, we have the EI in closed-form as:

$$\alpha^{EI}(x, p) = [\mu(x, p) - f^+] \times \Phi(z) + \sigma(x, p) \times \phi(z)$$

where $z = \frac{\mu(x, p) - f^+}{\sigma(x, p)}$ and f^+ is the best observed value up to the current iteration, $\Phi(z)$ is the standard normal cumulative distribution function and $\phi(z)$ is the standard normal probability density function. When the uncertainty is zero $\sigma(x, p) = 0$, the $\alpha^{EI}(x, p) = 0$.

Hyperparameters considerations

Personalized Bayesian optimization relies on a personalized Gaussian process surrogate model to select a next point for testing. This personalized GP model (defined in section 'Personalized

Gaussian process for joint modeling of target function and baseline ability'.) involves several hyperparameters including the length scales σ_l in Eq (5), σ_p in Eq (6), and the noise variance σ_n^2 in Eq (4). We make use of the property of the Gaussian process to estimate these hyperparameters directly from the observed data by maximizing the log marginal likelihood of a GP model [70]. For robustness, we have also normalized the input $x \in [0,1]^2$, $p \in [0,1]$ and standardized the output score $N(0,1)$ as popularly used in previous work [71]. Given this normalized space, the estimated hyperparameters vary by iterations within the range as follows $\sigma_l \in [0.03,0.4]$, $\sigma_p \in [0.07,0.5]$ and $\sigma_n^2 \in [0.01, 2]$.

One can optimize the EI [43,72] over the current best result or the GP-UCB. In short, it is more likely that the UCB selects evaluations with both a high mean and high variance. The EI and UCB have been shown to be efficient in the number of function evaluations required to find the global optimum of many multimodal black-box functions [43,73]. During the present study, the EI was applied to find the optimum in arithmetic performance. Lastly, we decided to remove one extreme drift rate value of 3.6 during the experimental procedure due to possible ceiling effects of the BO for sampling the same stimulation parameters. However, the inclusion of this data point did not significantly alter our results. For similar results without exclusion of this data point, see **S5 Fig**. In total, we acquired 148/150 iterations. In addition, due to technical problems another data point was not included in the BO procedure.

Simulation analysis

Simulations were run to validate the pBO procedure during arithmetic performance and tACS. This analysis aimed to show that pBO can outperform both a 'standard' BO algorithm and random sampling when identifying an optima in a noisy environment. Note that the present study contained three dimensions, namely frequency, current, and individualized baseline ability. Therefore, we utilized a Hartmann function [42] that included four local minima in three dimensions as an example, to enable our simulations to be comparable to our experimental data. As human-based studies are prone to noisy evaluations, we decided to introduce noise in the simulation by running the same Hartmann 3-dimensional function whilst adding different noise variation values (σ_n^2). The pBO algorithm presented in this work was compared to a standard BO algorithm which did not incorporate the personalized dimension into its evaluations, as well as a random sampling algorithm. Performance in these simulations was compared in terms of the best found value at each of the 60 iterations, as well as the distance from the known optima location with the Euclidean distance as a metric. Each simulation was repeated 30 times at each level of noise, and the three algorithm's mean performance and standard deviation over these repeats was calculated. Note that it is not possible to calculate the Euclidean distance between subsequent stimulation pairs due to the inclusion of a personalized variable.

EEG analysis of spectral power and frontoparietal theta connectivity

The rs-EEG data of the remaining datasets were separated in 2 second segments with an overlap of 1 second and windowed with a Hann window. Subsequently, data were transformed into the frequency domain via fast Fourier transformation (FFT). Theta (4–8 Hz) and beta (14–30 Hz) frequency bands were calculated according to their relative power (μV^2) and normalized by dividing the absolute frequency power of each frequency band by the average absolute power in the 1.5–30 Hz range. In addition, we also normalized the power by dividing the absolute frequency power by the average absolute power in the 4–50 Hz range. The weighted phase lag index (wPLI) in the theta and beta range was computed to determine the phase lag synchronization between the left frontal and parietal areas at baseline and after every tACS

block. This computation was made for the complementary channels F3 and P3. The theta wPLI was calculated for 4–8 Hz in steps of 1 Hz and the beta wPLI was calculated from 14–30 Hz in steps of 4 Hz. Furthermore, we normalized wPLI by calculating the wPLI at the applied tACS frequency divided by the baseline wPLI at the same frequency.

First, outliers were removed with Cook's distance before running statistical models. To focus on the relation between arithmetic baseline ability and spectral power, separate regression models were run with theta and beta power as dependent factors. Likewise, we tested whether there was a relation between frontoparietal theta and beta connectivity scores by running several regression models in steps of 1 Hz for theta wPLI and steps of 4 Hz for beta wPLI.

Statistical analysis

All the reported inferential statistical analysis was done with RStudio version 1.2.5042 with significance defined as $p \leq 0.05$ [74]. All data is presented as mean ± SD with n = 50 for electrophysiology analysis and n = 49 for the pBO analysis. Pre-processing of electrophysiological data was done with EEGLAB 13.6.5b [62] which is an open source toolbox running on MatlabR2018b [63]. Subsequently, normalized electrophysiological data was checked for outliers with Cook's distance and entered in log-transformed regression models using the stats package [74] with spectral power or connectivity measures as dependent variables and arithmetic baseline ability as independent variable. A correlation analysis on normally distributed datasets was run to calculate the bivariate Pearson's coefficient (r) to investigate differences in sensation and blinding, and a non-parametric (Spearman's rho (r_s)) correlation on non-normally distributed variables. Generalized linear mixed effects models (GLMM) were run with the nlme package [75] to explore EEG changes induced by tACS during arithmetic performance (see **S1 Text**). The pBO algorithm and simulations were run with Python version 3.6 [76], using the SciPy, NumPy and Scikit-learn libraries [77–79]. Note that no inferential statistics such as a GLMM is able to reliably investigate performance gains due to the inability to disentangle the exploration and exploitation trade-off of the pBO algorithm between blocks.

Supporting information

S1 Fig. Histogram plot showing the number of subjects in every baseline ability (n = 50). More subjects were on the lower part of the spectrum of the baseline ability range than the higher part.
(TIF)

S2 Fig. Side effects of different tACS current intensities. Different side-effects are shown according to the indicated sensation on a scale from 1–10 (n = 150 based on 50 subjects). 1 was indicated as a low sensation ('I did not feel the sensation') and 10 is a strong sensation ('I felt the sensation to a considerable degree'). The high value for fatigue at 0.1 mA is likely to be due to the low number of subjects (n = 2) who received this stimulation, and it might reflect a general state.
(TIF)

S3 Fig. Side effects of different tACS frequency intensities. Different side-effects are shown according to the indicated sensation on a scale from 1–10 (n = 150 based on 50 subjects). 1 was indicated as a low sensation ('I did not feel the sensation') and 10 is a strong sensation ('I felt the sensation to a considerable degree').
(TIF)

S4 Fig. Blinding efficacy of tACS. The figure shows the percentage of correct indications that stimulation was real for every applied current (n = 150 based on 50 subjects). Blinding efficacy

of tACS is at change level (~50%).
(TIF)

S5 Fig. Best found value of the personalized Bayesian optimization (pBO) procedure without exclusion of data point 46 (n = 50). Arithmetic performance in terms of drift rate for every best-found value for $f(x)$ and for every iteration of the pBO procedure during stimulation without exclusion of data point number 46.
(TIF)

S6 Fig. The interaction between EEG power, current, and frequency in predicting arithmetic performance for subjects with low arithmetic baseline ability (n = 25). Arithmetic performance (log transformed drift rates) during stimulation is shown on the y-axis and the normalized (post stimulation/pre stimulation) EEG power $\mu V^2/Hz$ (log transformed) based on the applied tACS frequency after stimulation is shown on the x-axis for four different tACS frequencies (4 Hz, 15 Hz, 30 Hz, and 50 Hz). Current intensity is indicated by the blue line (0.1 mA), the black line (1 mA), and the grey line (1.6 mA). Shaded areas indicate 95% confidence intervals. Note that different tACS categories and current intensities are presented for visualization purposes, to allow a better grasp of an interaction that is based on continuous variables.
(TIF)

S1 Table. Number of subjects (n) according to the different currents (mA) received in one stimulation block.
(DOCX)

S2 Table. Number of subjects (n) according to the different frequencies (Hz) received in one stimulation block.
(DOCX)

S3 Table. Fixed effects of the mixed effects model for arithmetic performance in low ability subjects (n = 25). Note: $^{**}p < 0.05$; $^{**}p < 0.01$.
(DOCX)

S4 Table. Fixed effects of the mixed effects model for arithmetic performance for high ability subjects (n = 24). Note: $^{**}p < 0.05$; $^{**}p < 0.01$.
(DOCX)

S1 Text. Supplementary results and discussion.
(DOCX)

S1 Mathematical Variables. All mathematical variables used in the present study clarified.
(DOCX)

S1 Questionnaire. Questionnaire items used to assess sensation levels during stimulation.
(DOCX)

Author Contributions

Conceptualization: Nienke E. R. van Bueren, Thomas L. Reed, Roi Cohen Kadosh.

Data curation: Nienke E. R. van Bueren.

Formal analysis: Nienke E. R. van Bueren, Thomas L. Reed, Vu Nguyen, James G. Sheffield, Roi Cohen Kadosh.

Funding acquisition: Nienke E. R. van Bueren, Roi Cohen Kadosh.

Investigation: Nienke E. R. van Bueren, Thomas L. Reed, Roi Cohen Kadosh.

Methodology: Nienke E. R. van Bueren, Thomas L. Reed, Vu Nguyen, Roi Cohen Kadosh.

Project administration: Nienke E. R. van Bueren, Thomas L. Reed, Roi Cohen Kadosh.

Resources: Nienke E. R. van Bueren, Thomas L. Reed, Roi Cohen Kadosh.

Software: Nienke E. R. van Bueren, Thomas L. Reed, Vu Nguyen, Roi Cohen Kadosh.

Supervision: Nienke E. R. van Bueren, Thomas L. Reed, James G. Sheffield, Sanne H. G. van der Ven, Michael A. Osborne, Evelyn H. Kroesbergen, Roi Cohen Kadosh.

Validation: Nienke E. R. van Bueren, Thomas L. Reed, Roi Cohen Kadosh.

Visualization: Nienke E. R. van Bueren, Thomas L. Reed, Vu Nguyen, Roi Cohen Kadosh.

Writing – original draft: Nienke E. R. van Bueren, Thomas L. Reed, Vu Nguyen, Roi Cohen Kadosh.

Writing – review & editing: Nienke E. R. van Bueren, Thomas L. Reed, Vu Nguyen, James G. Sheffield, Sanne H. G. van der Ven, Michael A. Osborne, Evelyn H. Kroesbergen, Roi Cohen Kadosh.

References

1. Sarkar A, Dowker A, Cohen Kadosh R. Cognitive enhancement or cognitive cost: trait-specific outcomes of brain stimulation in the case of mathematics anxiety. J Neurosci [Internet]. 2014 Dec 10 [cited 2017 Dec 1]; 34(50):16605–10. Available from: http://www.ncbi.nlm.nih.gov/pubmed/25505313 https://doi.org/10.1523/JNEUROSCI.3129-14.2014 PMID: 25505313

2. Looi CY, Duta M, Brem A-K, Huber S, Nuerk H-C, Cohen Kadosh R. Combining brain stimulation and video game to promote long-term transfer of learning and cognitive enhancement. Sci Rep [Internet]. 2016 Apr 23 [cited 2018 Jul 2]; 6(1):22003. Available from: http://www.ncbi.nlm.nih.gov/pubmed/26902664 https://doi.org/10.1038/srep22003 PMID: 26902664

3. Santarnecchi E, Muller T, Rossi S, Sarkar A, Polizzotto NR, Rossi A, et al. Individual differences and specificity of prefrontal gamma frequency-tACS on fluid intelligence capabilities. Cortex [Internet]. 2016 Feb 1 [cited 2019 Aug 31]; 75:33–43. Available from: https://www.sciencedirect.com/science/article/pii/S0010945215003810 https://doi.org/10.1016/j.cortex.2015.11.003 PMID: 26707084

4. Almquist JN-F, Mathan S, Brem A-K, Plessow F, McKanna J, Santarnecchi E, et al. FAST: A Novel, Executive Function-Based Approach to Cognitive Enhancement. Front Hum Neurosci [Internet]. 2019 Aug 2 [cited 2019 Aug 31]; 13:235. Available from: https://www.frontiersin.org/article/10.3389/fnhum.2019.00235/full PMID: 31427935

5. Yang L, Zhang W, Wang W, Yang Z, Wang H, Deng Z, et al. Neural and Psychological Predictors of Cognitive Enhancement and Impairment from Neurostimulation. Adv Sci [Internet]. 2020 Feb 21 [cited 2020 Jun 1]; 7(4):1902863. Available from: https://onlinelibrary.wiley.com/doi/abs/10.1002/advs.201902863 PMID: 32099765

6. Tseng P, Hsu T-Y, Chang C-F, Tzeng OJL, Hung DL, Muggleton NG, et al. Behavioral/Systems/Cognitive Unleashing Potential: Transcranial Direct Current Stimulation over the Right Posterior Parietal Cortex Improves Change Detection in Low-Performing Individuals. 2012 [cited 2019 Aug 31]; Available from: https://www.jneurosci.org/content/jneuro/32/31/10554.full.pdf

7. Harty S, Cohen Kadosh R. Suboptimal Engagement of High-Level Cortical Regions Predicts Random-Noise-Related Gains in Sustained Attention. Psychol Sci [Internet]. 2019 Jul 19 [cited 2019 Aug 31];095679761985665. Available from: http://journals.sagepub.com/doi/10.1177/0956797619856658 PMID: 31322974

8. Furuya S, Klaus M, Nitsche MA, Paulus W, Altenmüller E. Ceiling effects prevent further improvement of transcranial stimulation in skilled musicians. J Neurosci. 2014 Oct 8; 34(41):13834–9. https://doi.org/10.1523/JNEUROSCI.1170-14.2014 PMID: 25297109

9. Schork NJ. Personalized medicine: Time for one-person trials. Vol. 520, Nature. Nature Publishing Group; 2015. p. 609–11. https://doi.org/10.1038/520609a PMID: 25925459

10. Rothwell PM, Cook NR, Gaziano JM, Price JF, Belch JFF, Roncaglioni MC, et al. Effects of aspirin on risks of vascular events and cancer according to bodyweight and dose: analysis of individual patient

data from randomised trials. Lancet. 2018 Aug 4; 392(10145):387–99. https://doi.org/10.1016/S0140-6736(18)31133-4 PMID: 30017552

11. Aguado BA, Grim JC, Rosales AM, Watson-Capps JJ, Anseth KS. Engineering precision biomaterials for personalized medicine. Vol. 10, Science Translational Medicine. American Association for the Advancement of Science; 2018.

12. Antal A, Herrmann CS. Transcranial Alternating Current and Random Noise Stimulation: Possible Mechanisms. Neural Plast [Internet]. 2016 May 3 [cited 2018 Nov 19]; 2016:1–12. Available from: http://www.hindawi.com/journals/np/2016/3616807/ https://doi.org/10.1155/2016/3616807 PMID: 27242932

13. Battleday RM, Muller T, Clayton MS, Cohen Kadosh R. Mapping the Mechanisms of Transcranial Alternating Current Stimulation: A Pathway from Network Effects to Cognition. Front Psychiatry [Internet]. 2014 Nov 20 [cited 2019 Aug 31]; 5:162. Available from: http://journal.frontiersin.org/article/10.3389/fpsyt.2014.00162/abstract PMID: 25477826

14. Dayan E, Censor N, Buch ER, Sandrini M, Cohen LG. Noninvasive brain stimulation: from physiology to network dynamics and back. Nat Neurosci [Internet]. 2013 Jul 25 [cited 2018 Oct 25]; 16(7):838–44. Available from: http://www.nature.com/articles/nn.3422 https://doi.org/10.1038/nn.3422 PMID: 23799477

15. Lorenz R, Simmons LE, Monti RP, Arthur JL, Limal S, Laakso I, et al. Efficiently searching through large tACS parameter spaces using closed-loop Bayesian optimization. Brain Stimul. 2019; https://doi.org/10.1016/j.brs.2019.07.003 PMID: 31289013

16. Tervo AE, Metsomaa J, Nieminen JO, Sarvas J, Ilmoniemi RJ. Automated search of stimulation targets with closed-loop transcranial magnetic stimulation. Neuroimage. 2020 Oct 15; 220:117082. https://doi.org/10.1016/j.neuroimage.2020.117082 PMID: 32593801

17. Shahriari B, Swersky K, Wang Z, Adams RP, de Freitas N. Taking the Human Out of the Loop: A Review of Bayesian Optimization. Proc IEEE [Internet]. 2016 Jan [cited 2019 Aug 5]; 104(1):148–75. Available from: https://ieeexplore.ieee.org/document/7352306/

18. Stefanou MI, Baur D, Belardinelli P, Bergmann TO, Blum C, Gordon PC, et al. Brain state-dependent brain stimulation with real-time electroencephalography-triggered transcranial magnetic stimulation. J Vis Exp [Internet]. 2019 Aug 20 [cited 2021 May 25]; 2019(150):59711. Available from: www.jove.comurl:https://www.jove.com/video/59711 https://doi.org/10.3791/59711 PMID: 31498312

19. Cavagnaro DR, Pitt MA, Myung JI. Adaptive Design Optimization in Experiments with People. 2009.

20. Lesmes LA, Jeon ST, Lu ZL, Dosher BA. Bayesian adaptive estimation of threshold versus contrast external noise functions: The quick TvC method. Vision Res. 2006 Oct 1; 46(19):3160–76. https://doi.org/10.1016/j.visres.2006.04.022 PMID: 16782167

21. Cavagnaro DR, Pitt MA, Gonzalez R, Myung JI. Discriminating among probability weighting functions using adaptive design optimization. J Risk Uncertain. 2013 Nov 29; 47(3):255–89. https://doi.org/10.1007/s11166-013-9179-3 PMID: 24453406

22. Cheng AK, Ong S. Contextual Gaussian Process Bandit Optimization.

23. Krause B, Cohen Kadosh R. Not all brains are created equal: the relevance of individual differences in responsiveness to transcranial electrical stimulation. Front Syst Neurosci. 2014; 8:25. https://doi.org/10.3389/fnsys.2014.00025 PMID: 24605090

24. Datta A, Truong D, Minhas P, Parra LC, Bikson M. Inter-Individual Variation during Transcranial Direct Current Stimulation and Normalization of Dose Using MRI-Derived Computational Models. Front Psychiatry [Internet]. 2012 Oct 22 [cited 2020 Jun 1]; 3(OCT):91. Available from: http://journal.frontiersin.org/article/10.3389/fpsyt.2012.00091/abstract PMID: 23097644

25. Ritchie SJ, Bates TC. Enduring Links From Childhood Mathematics and Reading Achievement to Adult Socioeconomic Status. Psychol Sci [Internet]. 2013 Jul 2 [cited 2019 Dec 9]; 24(7):1301–8. Available from: http://journals.sagepub.com/doi/10.1177/0956797612466268 PMID: 23640065

26. Willmes K. Chapter 17 Acalculia. Vol. 88, Handbook of Clinical Neurology. 2008. p. 339–58. https://doi.org/10.1016/S0072-9752(07)88017-1 PMID: 18631700

27. Kaufmann L, Mazzocco MM, Dowker A, von Aster M, Göbel SM, Grabner RH, et al. Dyscalculia from a developmental and differential perspective. Front Psychol [Internet]. 2013 [cited 2017 Sep 3]; 4:516. Available from: http://www.ncbi.nlm.nih.gov/pubmed/23970870 https://doi.org/10.3389/fpsyg.2013.00516 PMID: 23970870

28. Parsons S., Bynner B. Does numeracy matter more? [Internet]. London: National Research and Development Centre for Adult Literacy and Numeracy; 2005 [cited 2017 Apr 14]. Available from: http://dera.ioe.ac.uk/22317/1/doc_2979.pdf

29. Artemenko C, Soltanlou M, Dresler T, Ehlis A-C, Nuerk H-C. The neural correlates of arithmetic difficulty depend on mathematical ability: evidence from combined fNIRS and ERP. Brain Struct Funct [Internet].

2018 Jul 10 [cited 2018 Nov 6]; 223(6):2561–74. Available from: http://link.springer.com/10.1007/s00429-018-1618-0 PMID: 29525887

30. Ischebeck A, Zamarian L, Egger K, Schocke M, Delazer M. Imaging early practice effects in arithmetic. Neuroimage [Internet]. 2007 Jul [cited 2017 Sep 3]; 36(3):993–1003. Available from: http://linkinghub.elsevier.com/retrieve/pii/S1053811907002248 https://doi.org/10.1016/j.neuroimage.2007.03.051 PMID: 17490893

31. Schroeder PA, Dresler T, Bahnmueller J, Artemenko C, Cohen Kadosh R, Nuerk H-C. Cognitive Enhancement of Numerical and Arithmetic Capabilities: a Mini-Review of Available Transcranial Electric Stimulation Studies. J Cogn Enhanc [Internet]. 2017 Mar 19 [cited 2017 Sep 3]; 1(1):39–47. Available from: http://link.springer.com/10.1007/s41465-016-0006-z

32. Grabner RH, Rütsche B, Ruff CC, Hauser TU. Transcranial direct current stimulation of the posterior parietal cortex modulates arithmetic learning. Eur J Neurosci [Internet]. 2015 Jul [cited 2018 Jul 8]; 42(1):1667–74. Available from: http://doi.wiley.com/10.1111/ejn.12947 PMID: 25970697

33. Hauser TU, Rotzer S, Grabner RH, Mérillat S, Jäncke L. Enhancing performance in numerical magnitude processing and mental arithmetic using transcranial Direct Current Stimulation (tDCS). Front Hum Neurosci [Internet]. 2013 Jun 6 [cited 2018 Jul 2]; 7:244. Available from: http://journal.frontiersin.org/article/10.3389/fnhum.2013.00244/abstract PMID: 23761750

34. Hauser TU, Rütsche B, Wurmitzer K, Brem S, Ruff CC, Grabner RH. Neurocognitive Effects of Transcranial Direct Current Stimulation in Arithmetic Learning and Performance: A Simultaneous tDCS-fMRI Study. Brain Stimul [Internet]. 2016 Nov 1 [cited 2018 Jul 4]; 9(6):850–8. Available from: https://www.sciencedirect.com/science/article/pii/S1935861X16301991 https://doi.org/10.1016/j.brs.2016.07.007 PMID: 27522169

35. Bieck SM, Artemenko C, Moeller K, Klein E. Low to No Effect: Application of tRNS During Two-Digit Addition. Front Neurosci [Internet]. 2018 Apr 5 [cited 2019 Jan 25]; 12:176. Available from: http://journal.frontiersin.org/article/10.3389/fnins.2018.00176/full PMID: 29674948

36. Klein E, Mann A, Huber S, Bloechle J, Willmes K, Karim AA, et al. Bilateral Bi-Cephalic Tdcs with Two Active Electrodes of the Same Polarity Modulates Bilateral Cognitive Processes Differentially. PLoS One. 2013 Aug 8; 8(8). https://doi.org/10.1371/journal.pone.0071607 PMID: 23951202

37. Popescu T, Krause B, Terhune DB, Twose O, Page T, Humphreys G, et al. Transcranial random noise stimulation mitigates increased difficulty in an arithmetic learning task. Neuropsychologia [Internet]. 2016 [cited 2017 Apr 23]; 81:255–64. Available from: http://www.sciencedirect.com.proxy.library.uu.nl/science/article/pii/S0028393215302682 https://doi.org/10.1016/j.neuropsychologia.2015.12.028 PMID: 26731199

38. Simonsmeier BA, Grabner RH, Hein J, Krenz U, Schneider M. Electrical brain stimulation (tES) improves learning more than performance: A meta-analysis. Neurosci Biobehav Rev [Internet]. 2018 Jan 1 [cited 2019 Jan 25]; 84:171–81. Available from: https://www.sciencedirect.com/science/article/pii/S0149763417303172 https://doi.org/10.1016/j.neubiorev.2017.11.001 PMID: 29128578

39. Sarkar A, Experimental RCK-CJ of, 2016 undefined. Transcranial electrical stimulation and numerical cognition. psycnet.apa.org [Internet]. [cited 2021 May 25]; Available from: https://psycnet.apa.org/journals/cep/70/1/41/

40. Wagenmakers E-J, Van Der Maas HLJ, Grasman RPPP. An EZ-diffusion model for response time and accuracy. Psychon Bull Rev [Internet]. 2007 Feb [cited 2019 Jun 21]; 14(1):3–22. Available from: http://link.springer.com/10.3758/BF03194023 PMID: 17546727

41. Aiken L, West S, Reno R. Multiple regression: Testing and interpreting interactions. 1991 [cited 2021 May 25]; Available from: https://books.google.com/books?hl=nl&lr=&id=LcWLUyXcmnkC&oi=fnd&pg=PP11&dq=Aiken,+West,+and+Reno+(1991)+&ots=fpdeUbYX2h&sig=3zfg-zp1bwRY7VcsuRXAHYhIrSI

42. Picheny V, Wagner T, Ginsbourger D. A benchmark of kriging-based infill criteria for noisy optimization. Struct Multidiscip Optim. 2013 Apr 21; 48(3):607–26.

43. Jones DR, Schonlau M, Welch WJ. Efficient Global Optimization of Expensive Black-Box Functions. J Glob Optim [Internet]. 1998 [cited 2019 Aug 10]; 13(4):455–92. Available from: http://link.springer.com/10.1023/A:1008306431147

44. Klimesch W. EEG alpha and theta oscillations reflect cognitive and memory performance: a review and analysis. Brain Res Rev [Internet]. 1999 Apr 1 [cited 2018 Nov 13]; 29(2–3):169–95. Available from: https://www.sciencedirect.com/science/article/pii/S0165017398000563 https://doi.org/10.1016/s0165-0173(98)00056-3 PMID: 10209231

45. Sauseng P, Griesmayr B, Freunberger R. Control mechanisms in working memory: A possible function of EEG theta oscillations. Neurosci Biobehav Rev [Internet]. 2010 Jun 1 [cited 2018 Nov 13]; 34(7):1015–22. Available from: https://www.sciencedirect.com/science/article/pii/S0149763409001973 https://doi.org/10.1016/j.neubiorev.2009.12.006 PMID: 20006645

46. Reinhart RMG, Nguyen JA. Working memory revived in older adults by synchronizing rhythmic brain circuits. Nat Neurosci [Internet]. 2019 May 8 [cited 2019 Jun 21]; 22(5):820–7. Available from: http://www.nature.com/articles/s41593-019-0371-x https://doi.org/10.1038/s41593-019-0371-x PMID: 30962628

47. Wang L, Gan JQ, Zhang L, Wang H. Differential recruitment of brain networks in single-digit addition and multiplication: Evidence from EEG oscillations in theta and lower alpha bands. Int J Psychophysiol [Internet]. 2018 Jun 1 [cited 2018 Nov 6]; 128:81–92. Available from: https://www.sciencedirect.com/science/article/pii/S0167876017304804 https://doi.org/10.1016/j.ijpsycho.2018.04.005 PMID: 29673650

48. Krause B, Dresler M, Looi CY, Sarkar A, Cohen Kadosh R. Neuroenhancement of High-Level Cognition: Evidence for Homeostatic Constraints of Non-invasive Brain Stimulation. J Cogn Enhanc. 2019 Feb 21; https://doi.org/10.1007/s41465-019-00126-7 PMID: 32190812

49. Fründ I, Ohl FW, Herrmann CS. Spike-timing-dependent plasticity leads to gamma band responses in a neural network. Biol Cybern. 2009 Sep; 101(3):227–40. https://doi.org/10.1007/s00422-009-0332-7 PMID: 19789891

50. Nunez PL. A Study of Origins of the Time Dependencies of Scalp EEG: II—Experimental Support of Theory. IEEE Trans Biomed Eng. 1981; BME-28(3):281–8. https://doi.org/10.1109/TBME.1981.324701 PMID: 7228074

51. Witkowski M, Garcia-Cossio E, Chander BS, Braun C, Birbaumer N, Robinson SE, et al. Mapping entrained brain oscillations during transcranial alternating current stimulation (tACS). Neuroimage. 2016 Oct 15; 140:89–98. https://doi.org/10.1016/j.neuroimage.2015.10.024 PMID: 26481671

52. Peters L, De Smedt B. Arithmetic in the developing brain: A review of brain imaging studies. Dev Cogn Neurosci [Internet]. 2018 [cited 2019 Apr 10]; 30:265–79. Available from: www.elsevier.com/locate/dcn https://doi.org/10.1016/j.dcn.2017.05.002 PMID: 28566139

53. Albert GC, Cook CM, Prato FS, Thomas AW. Deep brain stimulation, vagal nerve stimulation and transcranial stimulation: An overview of stimulation parameters and neurotransmitter release. Vol. 33, Neuroscience and Biobehavioral Reviews. Pergamon; 2009. p. 1042–60. https://doi.org/10.1016/j.neubiorev.2009.04.006 PMID: 19433105

54. Sisterson ND, Wozny TA, Kokkinos V, Constantino A, Richardson RM. Closed-Loop Brain Stimulation for Drug-Resistant Epilepsy: Towards an Evidence-Based Approach to Personalized Medicine. Vol. 16, Neurotherapeutics. Springer New York LLC; 2019. p. 119–27. https://doi.org/10.1007/s13311-018-00682-4 PMID: 30378004

55. Elias GJB, Namasivayam AA, Lozano AM. Deep brain stimulation for stroke: Current uses and future directions. Vol. 11, Brain Stimulation. Elsevier Inc.; 2018. p. 3–28. https://doi.org/10.1016/j.brs.2017.10.005 PMID: 29089234

56. Snowball A, Tachtsidis I, Popescu T, Thompson J, Delazer M, Zamarian L, et al. Long-Term Enhancement of Brain Function and Cognition Using Cognitive Training and Brain Stimulation. Curr Biol [Internet]. 2013 Jun [cited 2017 Sep 3]; 23(11):987–92. Available from: http://linkinghub.elsevier.com/retrieve/pii/S0960982213004867 https://doi.org/10.1016/j.cub.2013.04.045 PMID: 23684971

57. De Smedt B, Holloway ID, Ansari D. Effects of problem size and arithmetic operation on brain activation during calculation in children with varying levels of arithmetical fluency. Neuroimage [Internet]. 2011 Aug 1 [cited 2019 Feb 14]; 57(3):771–81. Available from: https://www.sciencedirect.com/science/article/pii/S1053811910016216 https://doi.org/10.1016/j.neuroimage.2010.12.037 PMID: 21182966

58. Ratcliff R, Smith PL, Brown SD, McKoon G. Diffusion Decision Model: Current Issues and History. Trends Cogn Sci [Internet]. 2016 Apr 1 [cited 2019 Aug 31]; 20(4):260–81. Available from: https://www.sciencedirect.com/science/article/abs/pii/S1364661316000255 https://doi.org/10.1016/j.tics.2016.01.007 PMID: 26952739

59. Kriegeskorte N, Simmons WK, Bellgowan PSF, Baker CI. Circular analysis in systems neuroscience: the dangers of double dipping. Nat Neurosci [Internet]. 2009 May 26 [cited 2019 Oct 17]; 12(5):535–40. Available from: http://www.nature.com/articles/nn.2303 https://doi.org/10.1038/nn.2303 PMID: 19396166

60. Snoek J, Larochelle H, Adams R. Advances in Neural Information Processing Systems. Practical Bayesian optimization of machine learning algorithms. 2012;2951–9.

61. Letham B, Karrer B, Ottoni G, Bakshy E. Constrained Bayesian optimization with noisy experiments. Bayesian Anal. 2019; 14(2):495–519.

62. Delorme A, Makeig S. EEGLAB: an open source toolbox for analysis of single-trial EEG dynamics including independent component analysis. J Neurosci Methods [Internet]. 2004 [cited 2017 Sep 25]; 134:9–21. Available from: https://sccn.ucsd.edu/eeglab/download/eeglab_jnm03.pdf https://doi.org/10.1016/j.jneumeth.2003.10.009 PMID: 15102499

63. MATLAB 2018b. Natick, Massachusetts: The MathWorks Inc.; 2018.

64. Amo C, Santiago L De, Barea R, López-Dorado A, Boquete L. Analysis of Gamma-Band Activity from Human EEG Using Empirical Mode Decomposition. mdpi.com [Internet]. [cited 2021 May 31]; Available from: www.mdpi.com/journal/sensors

65. Brennan AM, Williams LM, Harris AW. Intrinsic, task-evoked and absolute gamma synchrony during cognitive processing in first onset schizophrenia. Journal of psychiatric research. 2018; 99:10–21. https://doi.org/10.1016/j.jpsychires.2017.12.004 PMID: 29407283

66. Asamoah B, Khatoun A, Mc Laughlin M. tACS motor system effects can be caused by transcutaneous stimulation of peripheral nerves. Nat Commun [Internet]. 2019 Dec 17 [cited 2019 Sep 27]; 10(1):266. Available from: http://www.nature.com/articles/s41467-018-08183-w https://doi.org/10.1038/s41467-018-08183-w PMID: 30655523

67. Frank B, Harty S, Kluge A, Cohen Kadosh R. Learning while multitasking: short and long-term benefits of brain stimulation. Ergonomics [Internet]. 2018 Nov 2 [cited 2019 Aug 31]; 61(11):1454–63. Available from: https://www.tandfonline.com/doi/full/10.1080/00140139.2018.1563722 PMID: 30587084

68. Tesch M, Schneider J, Choset H. Learning Stochastic Binary Tasks using Bayesian Optimization with Shared Task Knowledge. 2013 Jun 1;

69. Srinivas N, Krause A, Kakade SM, Seeger M. Gaussian Process Optimization in the Bandit Setting: No Regret and Experimental Design. IEEE Trans Inf Theory [Internet]. 2009 Dec 20 [cited 2020 Feb 10]; 58 (5):3250–65. Available from: http://arxiv.org/abs/0912.3995

70. Rasmussen CK, Williams CK. Gaussian Processes for Machine Learning. 2006.

71. Nguyen V, Osborne MA. Knowing The What But Not The Where in Bayesian Optimization [Internet]. proceedings.mlr.press. 2020 [cited 2021 May 25]. Available from: http://proceedings.mlr.press/v119/nguyen20d.html

72. Paul S, Chatzilygeroudis K, Ciosek K, Mouret J-B, Osborne MA, Whiteson S. Alternating Optimisation and Quadrature for Robust Control [Internet]. Vol. 32, Proceedings of the AAAI Conference on Artificial Intelligence. 2018 Apr [cited 2021 May 25]. Available from: www.aaai.org

73. Bull AD. Convergence Rates of Efficient Global Optimization Algorithms. J Mach Learn Res [Internet]. 2011 [cited 2019 Aug 5]; 12(Oct):2879–904. Available from: http://www.jmlr.org/papers/v12/bull11a.html

74. R Core Team. R Foundation for statistical Computing. 2020 [cited 2021 May 25]; Available from: https://www.r-project.org

75. Pinheiro J, Bates D, DebRoy S, . . . DS-. R org/package=nlme. R package, 2020 undefined. R Development Core Team. nlme: Linear and nonlinear mixed effects models, 2012.

76. van Rossum G, Drake FL Jr. Python reference manual. Centrum voor Wiskunde en Informatica Amsterdam; 1995.

77. Virtanen P, Gommers R, Oliphant T, . . . MH-N, 2020 undefined. SciPy 1.0: fundamental algorithms for scientific computing in Python. nature.com [Internet]. [cited 2021 May 25]; Available from: https://www.nature.com/articles/s41592-019-0686-2?es_p=11046330

78. Harris C, Millman K, van der Walt S, Nature RG-, 2020 undefined. Array programming with NumPy. nature.com [Internet]. [cited 2021 May 25]; Available from: https://www.nature.com/articles/s41586-020-2649-2?fbclid=IwAR3qKNC7soKsJlgbF2YCeYQl90umdrcbM6hw8vnpaVvqQiaMdTeL2GZxUR0

79. Pedregosa F, Varoquaux G, Gramfort A, Michel V, Thirion B, Grisel O, et al. "Scikit-learn: Machine learning in Python." Journal of machine learning research 12 (Oct), 2825–2830.